The Cryosphere Discuss., 5, 307–338, 2011
www.the-cryosphere-discuss.net/5/307/2011/
doi:10.5194/tcd-5-307-2011

The Cryosphere Discussions

Scale-dependent measurement and analysis of ground surface temperature variability in alpine terrain

S. Gubler[1], J. Fiddes[1], S. Gruber[1], and M. Keller[2]

[1]Department of Geography, University of Zurich, Switzerland
[2]Computer Engineering and Networks Laboratory, ETH Zurich, Switzerland

Received: 23 December 2010 – Accepted: 4 January 2011 – Published: 25 January 2011

Correspondence to: S. Gubler (stefanie.gubler@geo.uzh.ch)

Published by Copernicus Publications on behalf of the European Geosciences Union.

Abstract

Measurements of environmental variables are often used to validate and calibrate physically-based models. Depending on their application, models are used at different scales, ranging from few meters to tens of kilometers. Environmental variables can vary strongly within the grid cells of these models. Validating a model with a single measurement is therefore delicate and susceptible to induce bias in further model applications.

To address the question of uncertainty associated with scale in permafrost models, we present data of 390 spatially-distributed ground surface temperature measurements recorded in terrain of high topographic variability in the Swiss Alps. We illustrate a way to program, deploy and refind a large number of measurement devices efficiently, and present a strategy to reduce data loss reported in earlier studies. Data after the first year of deployment is presented.

The measurements represent the variability of ground surface temperatures at two different scales ranging from few meters to some kilometers. On the larger scale, the dependence of mean annual ground surface temperature on elevation, slope, aspect and ground cover type is modelled with a linear regression model. Sampled mean annual ground surface temperatures vary from −4 °C to 5 °C within an area of 16 km^2 subject to elevational differences of approximately 1000 m. The measurements also indicate that mean annual ground surface temperatures vary up to 6 °C (i.e., from −2 °C to 4 °C) even within an elevational band of 300 m. Furthermore, variations can be high (up to 2.5 °C) at distances of less than 14 m in homogeneous terrain. The effect of this high variability of an environmental variable on model validation and applications in alpine regions is discussed.

TCD
5, 307–338, 2011

1 Introduction

The combination of environmental monitoring and modelling plays an important role when investigating today's and future climate and its impact on diverse phenomena of the cryosphere. Measurements are widely used for model validation and calibration. However, the problem of comparing model simulations made at one scale to measurements taken at another scale has no simple solution. The relevance of this issue increases when modelling phenomena such as snow cover on permafrost in highly variable terrain as the Swiss Alps.

The study of permafrost in mountain regions has become important in view of ongoing climate change (Harris et al., 2009; Gruber and Haeberli, 2007). Alpine environments are characterized by variable topography, influencing slope, aspect, elevation, ground properties, snow distribution and the energy fluxes at the Earth's surface. Ground temperatures thus vary over short distances and permafrost is highly influenced by this topographic variability.

Diverse permafrost studies have been performed in alpine regions in the last decades ranging from long-term monitoring projects such as Permafrost Monitoring Switzerland (PERMOS: www.permos.ch) over measurement campaigns of bottom temperature of snow (BTS) (Haeberli, 1973; Hoelzle et al., 2003) and ground surface temperatures (GST) (Gruber et al., 2004a; Hoelzle and Gruber, 2008) to statistical and physically based modelling (Haeberli, 1975; Stocker-Mittaz et al., 2002; Gruber, 2005; Nötzli et al., 2007). As mentioned before, the combination of measuring and modelling has great importance to enhance trust in model outcomes. The difficulties that arise from scaling issues can however be large: in contrast to measurements, spatially-distributed models are often grid-based and represent areas of several square meters to square kilometers. Since the physical processes that influence the pattern of variation of a phenomena operate and interact at different spatial scale, spatial variation can simultaneously occur on scales of different orders of magnitude (Oliver and Webster, 1986). Therefore, the extrapolation of results (including calibrated model outputs)

TCD
5, 307–338, 2011

based on point measurements requires caution, especially in highly variable terrain (Nelson et al., 1998). Due to the lack of spatially-distributed measurements, the influence of the scaling problem on model validation is barely investigated.

The aim of this study is to obtain and analyse a spatially-distributed and dense GST dataset in an alpine environment. Since GST is strongly coupled to air temperature, it depends, in a first approximation, on altitude. However, GST is also strongly influenced by topography through snow redistribution, exposition to the sun, shading from surrounding terrain and ground properties.

Snow cover exerts an important influence on the ground thermal regime based on differing processes (Zhang, 2005). On gently inclined Alpine slopes, snow cover mostly causes a net increase of mean annual ground surface temperatures (MAGST) due to its insulating effect during winter, but the timing and thickness of first snow cover, mean snow cover thickness as well as the timing of melt-out strongly control the local magnitude of this effect and are subject to strong inter-annual variation (Hoelzle et al., 2003; Brenning et al., 2005).

Near-surface material can also affect GST and induce a large lateral variability of GST over just tens of meters (e.g., Blackwell et al., 1980; Gruber and Hoelzle, 2008). Especially for coarse block material, a lowering of MAGST has been observed and can be attributed to the circulation of cold air during winter (Haeberli, 1973; Harris, 1996; Juliussen and Humlum, 2008) as well as purely conductive effects that do not require ventilation (Gruber and Hoelzle, 2008).

Furthermore, the exposition to solar radiation has a strong effect on the energy budget at a specific point. The amount of radiation received at a point depends strongly on slope angle, the exposure to the sun and shading from surrounding terrain and the difference in GST between two sides of an east-west oriented ridge can be more than 5 °C (Gruber et al., 2004b; PERMOS, 2010).

In this paper, we address the following questions:

– How can we efficiently obtain a spatially-distributed and dense set of measurements, that represent diverse scales of variability?

TCD
5, 307–338, 2011

– How do topographic parameters and ground cover types influence MAGST in an area of several square kilometers?

– What is the variation of ground temperatures within a 10 m×10 m field?

– What uncertainty is associated with scaling between point measurements and gridded models?

2 Instruments

Intensive networks used in spatially-distributed environmental monitoring requires inexpensive and simply deployable measurement devices. The iButton® DS1922L (Fig. 1) is a coin-sized, commercial device that integrates a micro-controller, 8 kB storage, a real-time clock, a temperature sensor, and a battery in a single package. The iButton measures temperatures from −40 °C to 85 °C with ±0.5 °C accuracy from −10 °C to 65 °C. At that resolution, it can store 4096 readings in memory.

iButtons are built in a durable stainless steel container rated "water resistant". A hydrophobic filter protects the sensor against dust, dirt, contaminants, water droplets and condensation. Lewkowicz (2008) states that about 13% of the iButtons that were deployed to monitor the snow-pack in Northern Canada failed, most probably due to water entry. To avoid this, iButtons were waterproofed by sealing them in pouches of 40 mm×100 mm (Fig. 2) in the present study. The material is a 140 µm thick laminate (oriented polyamide, polyethylene and aluminium) designed to withstand long periods of wetness as well as intense solar radiation without significant deterioration. Since the iButtons are buried into the ground, the pouches have no influence on the measured GST. Using a portable impulse tong sealer (polystar 300 A) operated with 12 V batteries, these pouches can be re-sealed in the field after cutting a seal and reading out the iButton data.

TCD
5, 307–338, 2011

3 Measurement campaign

3.1 Study site

The study site of Corvatsch lies in the eastern part of the Swiss Alps (Fig. 3). The northern part is a ski resort in winter. Several rock glaciers and some small glaciers exist around Piz Corvatsch, and the area has many times been a place for cryospheric research. A cable car facilitates the access to the area. Elevation ranges from approximately 1900 m to 3300 m a.s.l. Precipitation reaches mean values of 800 mm in the valley floors and 1000 mm to 2000 mm in the valley side belts (Schwarb et al., 2000). The elevation of the mean annual air temperature zero degrees isotherm is at 2200 m a.s.l. Meteo data is measured by MeteoSwiss at Piz Corvatsch in the center of the study area. The WGS84 coordinates of the station are 46.42 (Latitude) and 9.82 (Longitude).

3.2 Experiment design

The aim of this campaign is measuring GST and its variability at small to medium scales, i.e., within meters to distances of a few kilometers. The amount of samples required to adequately resolve the spatial patterns of the phenomena of interest is increases with to their heterogeneity (Nelson et al., 1998). In order to resolve the spatial patterns and the variability of GST around Corvatsch, 39 locations, so-called footprints, were selected such that most of the topographic variability within this area of 16 km^2 is represented (Fig. 3). On the one hand, the focus in footprint selection lay on the influence of topographic variables elevation, slope and aspect, and additionally ground cover types and terrain curvature. On the other hand, the replication of GST measurements within each 10 m×10 m footprint reflects the variability in GST at a very small scale. Each footprint is chosen to be as homogeneous as possible.

To represent GST variability due to slope, aspect and ground material, one main elevational band was selected for intense instrumentation. It ranges from 2600 m to

TCD
5, 307–338, 2011

2900 m a.s.l. Some footprints lie outside this band and reflect the dependence of GST on elevation. The footprints cover all aspects, steep and gentle slopes and different ground cover types such as meadow, fine material and coarse blocks (Tables 1 and 2). Aspect, slope and elevation were estimated from a lidar-derived digital surface model (Swissphoto) of 10 m resolution. Note that slopes which are larger than 50° are not samples in this study, since such steep terrain is hardly accessible and mostly consisting of rock faces which are not suitable for iButton-based measurement.

Shading from surrounding terrain plays a major role in determining the amount of solar radiation reaching the ground. At each footprint, the local horizon was recorded using a digital camera (Nikon Coolpix 990) with a fish eye converter (Nikon FC-E8) (Gruber et al., 2003).

3.3 Logger placement

In order to record near-surface temperatures and avoid heating by direct solar radiation, the iButtons were burried approximately 5 cm into the ground or placed between and underneath boulders. GST is measured every 3 h at 0.0625 °C resolution enabling operation for 512 days before the memory is full.

The 39 footprints were selected as described in Sect. 3.2. Within each 10 m×10 m footprint, we randomly distributed ten iButtons (Fig. 4). The one hundred square meters were numbered, and a uniform sample of size 10 was generated with the statistical programme R, determining the ten squares to place the iButtons. Random placement reduces systematic bias in the measurements due to subjectivity.

Each iButton was fixed to a yellow string to facilitate refinding. To prevent iButtons from falling down steep slopes, loggers were attached to large, stable boulders. The position of each iButton was additionally recorded using a differential GPS. At each footprint, a wooden stick was stamped into the ground, marking as one vertex of the 10 m×10 m square. Two blue ropes were attached to the stick identifying the local grid. All sticks were left in the ground ensuring the refinding of the footprints the following year.

TCD
5, 307–338, 2011

The iButtons were distributed in two field campaigns. Therefore, the two groups AA to AS (17 July 2009 to 16 July 2010, period 1) and AT to BM (14 August 2009 to 13 August 2010, period 2) cover slightly different time periods. The 3-hourly data recording always started at midnight.

3.4 Campaign automation

An iButton can be programmed and read out by connecting the device to a PC. At the beginning of a campaign, each device must be initially programmed by uploading a set of mission parameters such as the sampling interval, the starting time of the measurement and the desired measurement resolution.

A campaign with hundreds of devices asks for as much automation as possible, and generates a large amount of data that must be handled properly. The iAssist management tool (Keller et al., 2010) was developed to deploy, localize and maintain the iButton data loggers. Concretely, iAssist is a graphical user interface application that was especially designed for the mass programming and collection of iButton devices. A relational database is used to store measurements and meta data, i.e., GPS coordinates and pictures. The easy and reliable handling of the data with related meta information is thereby assured. The current version of the software runs on an Intel Atom netbook running Linux.

4 Data description and data analysis

In this section we present first results after one year of measurements. The data is used to estimate a) the inter-footprint variability due to topography at the medium scale (few kilometers) and b) the intra-footprint variability at a small scale (few meters) of MAGST.

In Sect. 4.1, we discuss data retrieval and data quality. In the following section, the measurements of some footprints are presented and qualitatively discussed. In

TCD
5, 307–338, 2011

Sect. 4.3, we analyse the inter-footprint variability of MAGST around the area of Corvatsch. For this, a linear regression model using the explanatory variables elevation, slope, aspect, ground cover type, terrain curvature and sky view factor is fitted to the data. In Sect. 4.4, the dependence of intra-footprint variability on the above mentioned variables is investigated, again by fitting a linear regression model.

4.1 Data quality

After the first year, 23 out of 390 iButtons could not be refound. Ten were lost due to the total removal of the footprint by a stranger, the remaining could not be refound in meadows. Every retrieved iButton recorded valid data, indicating the importance of the pouches used when compared to 13% loss reported previously (Lewkowicz, 2008). However, some iButtons reappeared on the surface (i.e., the measurements are disturbed by the direct solar radiation) and were excluded from the analysis. In total, 93% of the iButtons recorded data that could be used for the analysis.

A zero curtain, i.e., the effect of latent heat due to freezing or thawing soils, results in stable temperatures near 0 °C over extended time periods. Zero curtains were detected at several footprints (for example at the end of the snow season in both AX and BC, Fig. 5) and serve, in this study, to analyse the accuracy of the measurement devices. The zero curtains at each individual iButton were detected in a first step by using a threshold of the temperature deviation from zero degrees. Varying the threshold from 0.0625 °C to 0.25 °C in steps of 0.0625 °C indicated that variations of zero curtain periods within even very homogeneous footprints are large for the smallest threshold. When chosing a threshold of 0.125 °C, detected zero curtain periods become homogeneous. Choosing the larger two thresholds does not have a big influence on the detected zero curtain periods. This indicates that the iButtons measure temperatures at an accuracy of ±0.125 °C (i.e. two digital numbers) near zero degrees, which improves the accuracy stated by MAXIM, the producer of the iButton devices, by a factor of four.

TCD
5, 307–338, 2011

Mean annual air temperature (MAAT) differs by approximately 0.16 °C between the two periods 1 and 2 (according to the meteo data taken at the top of Corvatsch by MeteoSwiss). To analyse the influence of this difference in MAAT, a linear regression model was fitted to the mean of the data from the overlapping time period (14 August 2009 to 16 July 2010) instead of the MAGST (the regression model fitted to the MAGST is found in Eq. 3). By this change, only the intercept of the linear regression model is modified, indicating that air temperature has an effect on absolute, but not on relative MAGST. Important differences in the snow cover were not observed when distributing or reading-out the iButtons.

4.2 General description

In Fig. 5, ground surface temperatures of four different footprint are presented. The grey lines in the background plot a maximum of ten iButtons located at the footprints. The red line indicates the mean GST at each time step. At the bottom of each plot, the range of all iButtons is plotted, indicating the temperature variability within each footprint. Snow cover is indicated in blue and was estimated manually. Danby and Hik (2007) presented an algorithm to determine snow cover based on daily temperature variations.

GST vary strongly at different footprints, depending on elevation, exposition to the sun and conditions of snow. The two footprints on top station of Corvatsch, AD and AJ, are highly correlated to air temperature, even in winter (Fig. 5). Both footprints are located at the sides of the ridge close to Corvatsch upper station. They are wind exposed and snow is less likely to accumulate. AJ, which is oriented to the east, shows bigger daily temperature amplitudes and is two degrees warmer than AD, which is west exposed. Since clouds often develop in the afternoon, the west exposed footprint AD receives less direct solar radiation.

The footprints BC and AX are snow covered during winter. Daily temperature variations cease in the beginning of October, when the first large snow fall event of winter 2009/2010 occurred. At BC, a very steep north-oriented slope, temperature damping

TCD
5, 307–338, 2011

by snow is observed some weeks later than at AX. In late spring, the snow cover at BC lasts much longer. Since the slope is north exposed, it receives very little solar radiation, and therefore snow melting occurs much slower than at the nearby, south-oriented slope AX. The difference in MAGST between AX in BC is more than 4 °C. At AX, GST in summer is much higher than at BC, and thus the combined effect of warming due to solar radiation at AX and cooling due to long lasting snow in late spring at BC are responsible for this large difference. This descriptive example shows the influence of topography on ground temperatures in high alpine areas very clearly.

Similar effects can be observed at diverse other footprints, for example at BA and AY. They lie very close together, however AY is in a zone with high snow accumulation. Melting takes much more time, and snow cover in AY lasts approximately one month longer than at BA, resulting in a 1.5 °C lower MAGST.

4.3 Inter-footprint variability

MAGST μ_k of footprint k is defined as the mean of the mean of each time series within that footprint, i.e.:

$$\mu_k := \frac{1}{B_k} \sum_{i=1}^{B_k} \mu_{k,i} \,. \tag{1}$$

Here, B_k is the number of iButtons at footprint k, and

$$\mu_{k,i} := \frac{1}{8 \cdot 365} \sum_{j=1}^{8 \cdot 365} T_{k,i,j} \,, \tag{2}$$

where $T_{k,i,j}$ denotes the jth measurement of the ith iButton.

Measured MAGST varies from −3.65 °C to 5.42 °C around Corvatsch (Tables 1 and 2). This variation can, to a large degree, be explained with the topographic variability. In order to quantify the influence of the topographic variables, a linear regression model was fitted using ordinary least squares. Spatial autocorrelation was not taken

TCD
5, 307–338, 2011

into account, since the variability due to the high variations in topography at very small distances dominates over spatial structures (Nelson et al., 1998). The full model contained the explanatory variables elevation, slope, aspect, ground cover type, sky view factor and curvature. An iterative, step-wise model reduction according to the Akaike-Information-Criteria (Akaike, 1973) combined with the addition of higher polynomials led to the model shown in Eq. (3). Interaction terms were not taken into account. Note that the cosine of the aspect is taken to ensure continuity, the addition of one allowed to model the quadratic dependence.

$$\begin{aligned}\mu_k = {} & 19.28 - 0.0055 \cdot \mathrm{Elevation}_k \\ & -0.83 \cdot (\cos(\mathrm{Aspect}_k) + 1)^2 \\ & -0.028 \cdot \mathrm{Slope}_k \\ & +0.25 \cdot \mathrm{dGCT}_{k,2} \\ & -2.13 \cdot \mathrm{dGCT}_{k,3} \\ & +\varepsilon_k \,.\end{aligned} \tag{3}$$

Note that GCT is a categorical variable and is therefore represented through the dummy variable dGCT (i.e., $\mathrm{dGCT}_{k,2}$=1 if and only if footprint k is of ground cover type 2, else $\mathrm{dGCT}_{k,2}$=0). Consequently, the different ground cover types influence the intercept of the linear regression. Recall that the random variables ε_k are independent, normally distributed with zero mean and constant variance. Residual analysis did not show any strong deviations from the model assumptions. The confidence interval of a coefficient contains all values that would not be rejected by the t-test at a previously specified significance level, i.e., it indicates the uncertainty associated with the coefficient. The 95% confidence intervals of Model (Eq. 3) are presented in Table 3. Since the data sample is relatively small (forty values fitted to four explanatory variables), some confidence intervals are quite large, for example the intercept. However, all variables (except dGCT_2 which, as part of a dummy variable, is not separable from the highly significant dGCT_3) differ significantly from zero. Sign and order of magnitude of the influence of a topographic variable on MAGST of Model (Eq. 3) are therefore valid.

TCD
5, 307–338, 2011

MAGST plotted against elevation is shown in Fig. 7. Additionally, the fitted values of Model (3) are plotted. The model explains 87% of the MAGST variability (Fig. 8), the model is highly significant ($p<10^{-13}$, where p is the p-value).

As mentioned in Sect. 4.1, the influence of the different time periods 1 and 2 on the regression analysis was analysed. Therefore, the linear regression model was fitted to the mean ground surface temperatures of the overlapping time periods. The only difference observed between the two analyses is a negative shift of the intercept of approximately 0.6 °C, resulting from the absent summer temperatures between the 17 July and the 13 August of the respective years.

4.4 Intra-footprint variability

The variability ξ_k of MAGST of footprint k is defined as the range of the MAGST of all iButtons within that footprint:

$$\xi_k := \max_{i=1,\cdots,B_k}(\mu_{k,i}) - \min_{i=1,\cdots,B_k}(\mu_{k,i}). \quad (4)$$

Variability in MAGST varies strongly between the different footprints. It ranges from 0.16 °C at the very homogeneous footprint AV to almost 2.5 °C at BH (Tables 1 and 2). Variation is generally larger for greater heterogeneity (Fig. 6). Similarly as above, we modeled the dependence of variation on the topographic variables. The final model is:

$$\begin{aligned}\log(\xi_k) = {} & -1.07 + 0.0007 \cdot \mathrm{Slope}_k^2 \\ & + 0.26 \cdot \mathrm{dGCT}_{k,2} \\ & + 0.88 \cdot \mathrm{dGCT}_{k,3} \\ & + \varepsilon_k .\end{aligned} \quad (5)$$

Again, model assumptions are not violated, the model however only explains 41% of the total variability in the range. The model is significant ($p<0.0003$). The confidence intervals of the linear model are shown in Table 4.

TCD
5, 307–338, 2011

5 Discussion

The techniques developed to protect, manage, distribute and refind many data loggers have proven to be effective. iAssist was especially useful for rapid (re-)programming of the iButtons in the field, and for the automatic storage of the data. In order to refind the buttons, mainly the yellow strings and the local grids were of great help. The pouches ensured a 100% success of data retrieval. The study has furthermore shown that the accuracy of the iButton is better (i.e., $\pm 0.125\,^{\circ}\mathrm{C}$) than stated by the producer. This was shown through the detection and analysis of zero curtains.

While our measurements have a high reliability due to their spatial density, their temporal support of only one full year needs to be kept in mind. As previous studies have demonstrated considerable inter-annual variability of ground temperatures (Hoelzle et al., 2003; Gruber et al., 2004a; Brenning et al., 2005) depending especially on snow conditions, absolute values need to be interpreted with caution.

MAGST decreases with a lapse rate of $-5.5\,^{\circ}\mathrm{C\,km^{-1}}$. While this overall value lies within the range of MAAT lapse rates reported for the Alps by Rolland (2002) and MAGST lapse rates of $-4\,^{\circ}\mathrm{C\,km^{-1}}$ to $-7\,^{\circ}\mathrm{C\,km^{-1}}$ found in the literature (Powell et al., 1988; Šafanda, 1999), it should not indicate that ground temperature gradient are exclusively tied to those of the air. The complex coupling between atmosphere and subsurface can results in markedly differing lapse rates depending on ground type, topography and snow cover.

Many of the footprints are located between 2600 m and 2900 m. We see in Fig. 7 that MAGST varies from $-2.4\,^{\circ}\mathrm{C}$ to $3.7\,^{\circ}\mathrm{C}$ within that elevational band. This variation cannot be explained with elevation alone (the linear model with only one predictor variable elevation reached an R^2 of 0.3). As we have seen in Model (Eq. 3), MAGST also strongly depends on the exposition to the sun and the ground classification, and to a smaller degree on the slope. Exposition to sun has a large influence, resulting in a difference of $3\,^{\circ}\mathrm{C}$ between north and south facing slopes. While this is a considerable difference, it is lower than that reported for steep rock (cf., Gruber et al., 2004a; PERMOS, 2010)

TCD
5, 307–338, 2011

due to the reduced differentiation between north and south and the effect of snow cover in more gently inclined slopes.

Near-surface material has a strong influence on MAGST that is around 2 °C smaller in coarse blocks than at meadow sites (cf., Hoelzle et al., 2003; Gruber and Hoelzle, 2008).

The variability of GST was defined as the range of the MAGST at one footprint. The analysis of the intra-footprint variability (Model Eq. 5) indicates that MAGST is more variable in coarse blocks and in steep terrain. Especially in homogeneous grass sites, variability is very small. Within coarse blocks, logger placement probably also has an effect on intra-footprint variability due to the difficulty of defining the surface. Snow distribution affects MAGST variability strongly, and is likely to be more variable at steep slopes and in rough terrain.

Due to the large differences in elevation, measured MAGST varies up to 9 °C in an area of approximately 16 km^2 in this study. But even within one elevational band (i.e., between 2600 m and 2900 m), MAGST differ more than 6 °C at locations of different expositions, slopes and ground cover materials. Validation or calibration of a grid-based model of 4 km resolution with one measurement taken within one grid cell is therefore very sensitive to the position of the measurement.

Even if a model is spatially highly resolved, variations of environmental variables can still be large within the grid cells. In this study, MAGST varies more than 2 °C within a homogeneous 100 m^2 field consisting of large boulders (i.e., BH) or which is steep (i.e., BG).

The results of this study confirm that the comparison of model outputs with measurements requires caution, especially when differences in scale are present. The estimation of scale-dependent variability of environmental variables is important for reliable model validation and calibration. The question how well a measurement represents its surroundings is essential. The availability of spatially-distributed measurements, such as the measurements presented in this study, facilitates the estimation of uncertainties associated with scaling issues and the planning of efficient measurement campaigns.

TCD
5, 307–338, 2011

6 Conclusions

The use of iButtons to intensively measure spatially-distributed GST was successful and pouches have shown to be very important. iButtons measure temperature with an accuracy of ±0.125 °C. The iAssist management tool is of great use for quick programming, campaign automation and storage of large volumes of data. The experiment design was effective for investigating the dependence of GST on topography, and to study small scale variability of GST.

Variations in MAGST can statistically be explained with the variables elevation, slope, aspect and ground cover type. In our measurements, MAGST are up to 2 °C higher in soil than within coarse blocks. South exposed slopes are in general 3 °C warmer than north facing slopes. Curvature of the terrain and the sky view factor had no significant influence in this model. Over the whole study area, measured MAGST variations go up to 9 °C.

MAGST vary also at very small scales: even in homogeneous areas, variations amount to more than 2.5 °C at distances of less than $\sqrt{2}\cdot 10\,\mathrm{m} \approx 14\,\mathrm{m}$ at steep slopes or in terrain of coarse blocks. Note that this is one fourth of the variation encountered over the whole study area.

This study shows that validation and calibration of grid-based models using measurements has to be performed with caution. The question of representativeness of a measurement location for its surroundings is often unclear. Since environmental variables vary strongly at even very small scales, model validation and calibration with measurements of these variables can strongly be biased. Repeated measuring at different scales allows to estimate the natural variability of a variable, and thereby to improve model validation.

TCD
5, 307–338, 2011

Appendix A

Data availability

The measurements, the meta data and the source code of the presented statistical analyses will be published on a webpage together with the final paper. At the moment, the reviewers are asked to obtain the data through the editor if desired. The data is ordered according to the footprint names (i.e., all measurements taken at footprint AA are found in the file data_AA.csv). Each file contains the temperature measurements of all iButtons that were placed within that footprint together with the time stamps. The file Footprint_Metadata.csv contains the meta data shown in Tables 1 and 2 plus sky view factor and different curvature indices. Additionally, a horizon file of each footprint is given (the horizon file of footprint AA is called hor_AA.csv, for example). The second column in the horizon file indicates the elevation of the surrounding terrain above the horizon in direction of the azimuth given in the first column.

Supplementary material related to this article is available online at: http://www.the-cryosphere-discuss.net/5/307/2011/tcd-5-307-2011-supplement.zip.

Acknowledgements. The authors are grateful for the support given by the Corvatschbahnen, the developers of iAssist Guido Hungerbühler, Oliver Knecht and Suhel Sheikh, as well as Vanessa Wirz, Christina Lauper and Marc-Olivier Schmid and everybody else who helped to distribute and refind the iButtons. This project was funded by the Swiss National Science Foundation (SNSF) via the NCCR MICS project PermaSense and the project CRYOSUB (Mountain Cryosphere Subgrid Parameterization and Computation, 200021_121868). All statistical analyses were performed with R (www.cran.r-project.org).

TCD
5, 307–338, 2011

References

Akaike, H.: A new look at the statistical model indentification, IEEE T. Automat. Contr., 19, 716–723, 1973. 318

Blackwell, D. D., Steele, J. L., and Brott, C. A.: The terrain effect on terrestrial heat flow, J. Geophys. Res., 85, 4757–4772, 1980. 310

Brenning, A., Gruber, S., and Hoelzle, M.: Sampling and statistical analyses of BTS measurements, Permafrost Periglac., 16, 383–393, 2005. 310, 320

Danby, R. K. and Hik, D. S.: Responses of white spruce (*Picea Glauca*) to experimental warming at a subarctic alpine treeline, Glob. Change Biol., 13, 437–451, 2007. 316

Gruber, S.: Mountain permafrost: transient spatial modelling, model verification and the use of remote sensing, Ph.D. thesis, University of Zurich, 2005. 309

Gruber, S. and Haeberli, W.: Permafrost in steep bedrock slopes and its temperature-related destabilization following climate change, J. Geophys. Res., 112, doi:10.1029/2006JF000547, 2007. 309

Gruber, S. and Hoelzle, M.: The cooling effect of coarse blocks revisited: a modeling study of a purely conductive mechanism, in: Proceedings of the 9th International Conference on Permafrost, Fairbanks, USA, 9th International Conference on Permafrost, 557–561, 2008. 310, 321

Gruber, S., Peter, M., Hoelzle, M., Woodhatch, I., and Haeberli, W.: Surface temperatures in steep alpine rock faces – a strategy for regional-scale measurement and modelling, Proceedings of the 8th International Conference on Permafrost 2003, Zürich, 325–330, 2003. 313

Gruber, S., Hoelzle, M., and Haeberli, W.: Permafrost thaw and destabilization of alpine rock walls in the hot summer of 2003, Geophys. Res. Lett., 31, doi:10.1029/2004GL0250051, 2004a. 309, 320

Gruber, S., King, L., Kohl, T., Herz, T., Haeberli, W., and Hoelzle, M.: Interpretation of geothermal profiles perturbed by topography: the alpine permafrost boreholes at Stockhorn plateau, Switzerland, Permafrost Periglac., 15, 349–357, 2004b. 310

Haeberli, W.: Die Basis-Temperatur der winterlichen Schneedecke als möglicher Indikator für die Verbreitung von Permafrost in den Alpen, Z. Gletscherk. Glaziol., 9, 221–227, 1973. 309, 310

Haeberli, W.: Untersuchung zur Verbreitung von Permafrost zwischen Flüelapass und Piz Gri-

TCD
5, 307–338, 2011

aletsch (Graubünden), Ph.D. thesis, Universitiy of Basel, 1975. 309
Harris, C., Arenson, L. U., Christiansen, H. H., Etzelmüller, B., Frauenfelder, R., Gruber, S., Haeberli, W., Hauck, C., Hölzle, M., Humlum, O., Isaksen, K., Kääb, A., Kern-Lötschg, M. A., Lehning, M., Matsuoka, N., Murton, J. B., Nötzli, J., Phillips, M., Ross, N., Seppälä, M., Springman, S. M., and Vonder Mühll, D.: Permafrost and climate in Europe: monitoring and modelling thermal, geomorphological and geotechnical responses, Earth-Sci. Rev., 92, 117–171, doi:10.1016/j.earscirev.2008.12.002, 2009. 309
Harris, S. A.: Lower mean annual ground temperature beneath a block stream in the Kunlun Pass, Qinghai Province, China, in: Proceedings of the Fifth Chinese Permafrost Conference, Lanzhou, 227–237, 1996. 310
Hoelzle, M. and Gruber, S.: Borehole and ground surface temperatures and their relationship to meteorological conditions in the Swiss alps, Proceedings of the 9th International Conference on Permafrost, Fairbanks, USA, 723–728, 2008. 309
Hoelzle, M., Haeberli, W., and Mittaz, C.: Miniature ground temperature data logger measurements 2000–2002 in the Murtèl-Corvatsch area, Eastern Swiss Alps, in: 8th International Conference on Permafrost, Proceedings, edited by: Phillips, M., Springman, S., and Arenson, L., Swets & Zeitlinger, Lisse, Zürich, 419–424, 2003. 309, 310, 320, 321
Juliussen, H. and Humlum, O.: Thermal regime of openwork block fields on the mountains Elahogna and Solen, Central-Eastern Norway, Permafrost Periglac., 19, 1–18, doi:10.1002/ppp.607, 2008. 310
Keller, M., Hungerbühler, G., Knecht, O., Skeikh, S., Beutel, J., Gubler, S., Fiddes, J., and Gruber, S.: iAssist: rapid deployment and maintenance of tiny sensing systems, 8th ACM Conference on Embedded Networked Sensor Systems, Zürich, 2010. 314
Lewkowicz, A. G.: Evaluation of miniature temperature-loggers to monitor snowpack evolution at mountain permafrost sites, Northwestern Canada, Permafrost Periglac., 19, 323–331, 2008. 311, 315
Nelson, F. E., Hinkel, K. M., Shiklomanov, N. I., Mueller, G. R., Miller, L. L., and Walker, D. A.: Active-layes thickness in North Central Alaska: systematic sampling, scale, and spatial autocorrelation, J. Geophys. Res., 103, 28963–28973, 1998. 310, 312, 318
Nötzli, J., Gruber, S., Kohl, T., Salzmann, N., and Haeberli, W.: Three-dimensional distribution and evolution of permafrost temperatures in idealized high-mountain topography, J. Geophys. Res., 112, doi:10.1029/2006JF000545, 2007. 309
Oliver, M. A. and Webster, M.: Combining nested and linear sampling for determining the scale

TCD
5, 307–338, 2011

and form of spatial variation of regionalized variables, Geogr. Anal., 18, 227–242, 1986. 309
PERMOS: Permafrost in Switzerland 2006/2007, in: Glaciological Report (Permafrost) No. 8/9 of the Cryospheric Commission of the Swiss Academy of Sciences, edited by Nötzli, J. and Vonder Mühll, D., 2010. 310, 320
Powell, W. G., Chapman, D. S., Balling, N., and Beck, A. E.: Handbook of terrestrial heat-flow density determination: with guidelines and recommendations of the International Heat Flow Commission, chap. Continental heat-flow density, Kluwer Academic Publishing, 167–222, 1988. 320
Rolland, C.: Spatial and seasonal variations of air temperature lapse rates in alpine regions, J. Climate, 16, 1032–1046, 2002. 320
Schwarb, M., Frei, C., Schär, C., and Daly, C.: Mean annual precipitation throughout the European Alps 1971–1990, National Hydrologic Service, Bern, Hydrological Atlas of Switzerland, 2000. 312
Stocker-Mittaz, C., Hoelzle, M., and Haeberli, W.: Modelling alpine permafrost distribution based on energy-balance data: a first step, Permafrost Periglac., 13, 271–282, 2002. 309
Šafanda, J.: Ground surface temperature as a function of the slope angle, Tectonophysics, 360, 367–375, 1999. 320
Zhang, T.: Influence of the seasonal snow cover in the ground thermal regime: an overview, Rev. Geophys., 43, doi:10.1029/2004RG000157, 2005. 310

TCD
5, 307–338, 2011

Table 1. Meta data of footprints. B_k denotes the number of valid iButton measurements at footprint k. MAGST of footprint k is denoted by $\mu_k := \frac{1}{B_k} \sum_{i=1}^{B_k} \mu_{k,i}$ and the variability of MAGST is $\xi_k := \max_{i=1,\cdots,B_k}(\mu_{k,i}) - \min_{i=1,\cdots,B_k}(\mu_{k,i})$. Coordinates are given in the Swiss coordinate system CH1903. Elevation, slope and aspect are derived from a Swissphoto DEM with 10 m resolution. Slope is given in degrees, as well as aspect counting from the north clockwise. GCT stands for ground cover type and classifies the footprints into three groups: group one is fine material often including organic material, group three is very coarse material such as the large boulders on the rock glaciers, and group two lies in between. Note that both footprints AL and AO are separated into two groups. Within AL, half of the iButtons lie in slightly concave terrain (AL1), the rest in convex terrain (AL2) on a ridge. Due to this difference which influences snow accumulation, AL1 and AL2 are treated as two different footprints. Similarly within AO: the ten iButtons are located on both sides of a steep N-S ridge, i.e., five iButtons are west-exposed, five are east-exposed.

Footprint	x-coord	y-coord	B_k	Elev.	Slope	Aspect	GCT	μ_k	ξ_k
AA	783 292	144 769	10	2694	38	251	1	3.82	0.59
AB	783 691	144 709	10	2745	16	96	2	2.96	1.33
AC	783 701	144 704	10	2743	31	112	2	4.34	1.15
AD	783 092	143 454	10	3303	29	263	3	−3.65	1.69
AE	783 490	144 696	10	2826	29	290	1	0.89	1.88
AF	782 888	144 552	10	2689	23	9	3	−1.62	2.12
AG	783 159	144 979	9	2664	48	243	2	2.29	2.52
AH	783 151	144 735	10	2663	9	318	3	−0.55	1.10
AI	782 437	145 612	7	2307	18	330	1	3.17	0.36
AJ	783 108	143 449	10	3302	27	113	3	−1.56	2.22
AL1	783 506	144 714	5	2824	14	347	2	1.00	0.22
AL2	783 506	144 714	5	2824	25	60	2	1.53	0.16
AM	783 682	144 727	10	2738	30	333	2	0.52	0.87
AN	783 155	145 070	9	2673	25	252	1	3.24	0.27
AO1	783 446	144 834	5	2811	36	64	3	−1.43	1.72
AO2	783 446	144 834	5	2811	18	238	3	1.41	0.60
AP	782 667	145 339	5	2405	15	335	1	2.56	0.45
AQ	783 135	144 517	10	2729	29	12	3	−1.04	1.06

TCD
5, 307–338, 2011

Table 2. Meta data of footprints.

Footprint	x-coord	y-coord	B_k	Elev.	Slope	Aspect	GCT	μ_k	ξ_k
AR	783 026	145 559	7	2528	28	288	1	2.91	0.25
AS	781 936	146 051	8	2100	35	315	1	4.89	1.09
AT	784 575	143 872	10	2790	36	100	2	3.52	1.00
AU	784 625	143 751	10	2773	33	88	3	1.67	0.55
AV	781 263	141 412	10	2538	0	212	1	3.59	0.16
AW	782 960	144 519	9	2700	19	333	3	−2.01	0.63
AX	781 380	142 736	10	2810	23	135	2	3.55	1.03
AY	782 264	143 661	10	2687	9	328	1	2.12	0.8
AZ	784 433	143 592	10	2876	7	61	2	2.41	0.28
BA	782 231	143 669	10	2697	27	111	1	3.60	0.44
BB	784 659	143 858	10	2763	14	103	1	3.06	0.45
BC	781 437	142 806	8	2783	41	357	2	−1.24	1.00
BD	782 420	143 906	10	2705	27	247	2	3.56	0.81
BE	781 543	142 558	9	2710	29	167	1	3.98	0.73
BF	781 972	143 576	10	2645	5	31	2	2.43	0.65
BG	782 351	144 237	10	2715	43	246	1	3.56	2.14
BH	781 525	142 480	10	2693	6	243	3	1.42	2.47
BI	779 993	142 631	4	2362	24	192	1	5.42	0.36
BJ	783 961	143 517	10	2997	36	90	2	1.46	1.24
BK	782 731	144 532	9	2691	31	355	2	1.69	0.46
BL	783 962	143 526	10	2875	19	35	2	0.21	1.01
BM	782 444	144 464	10	2715	44	314	2	−1.49	2.26

TCD
5, 307–338, 2011

Table 3. 95% confidence intervals of the inter-footprint analysis coefficients (Model Eq. 3).

Coefficient	2.5%	97.5%
Intercept	14.79	23.77
Elevation	−0.0072	−0.0038
$(\cos(\text{Aspect})+1)^2$	−1.02	−0.62
Slope	−0.052	−0.003
$dGCT_2$	−0.52	1.01
$dGCT_3$	−3.01	−1.25

TCD
5, 307–338, 2011

Table 4. 95% confidence intervals of the intra-footprint analysis coefficients (Model Eq. 5).

Coefficient	2.5%	97.5%
Intercept	−1.49	−0.66
$Slope^2$	0.0003	0.001
$dGCT_2$	−0.21	0.72
$dGCT_3$	0.36	1.4

TCD
5, 307–338, 2011

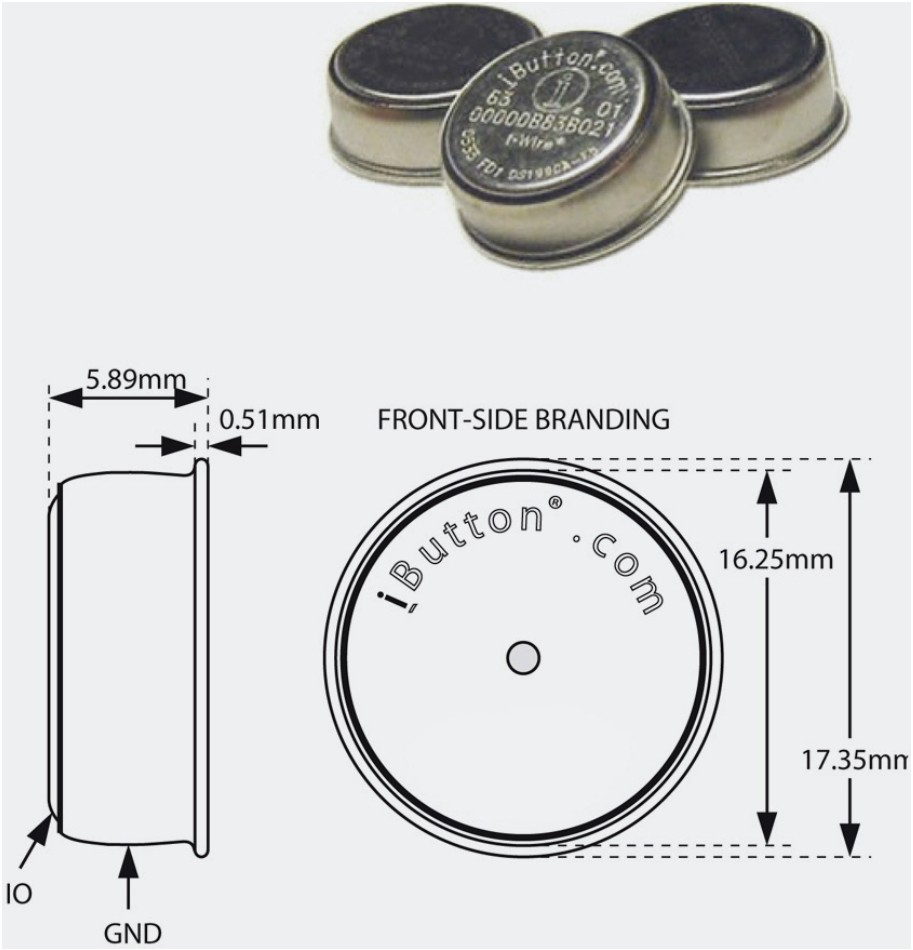

Fig. 1. The iButton® DS1922L that was used for temperature measurements.

TCD
5, 307–338, 2011

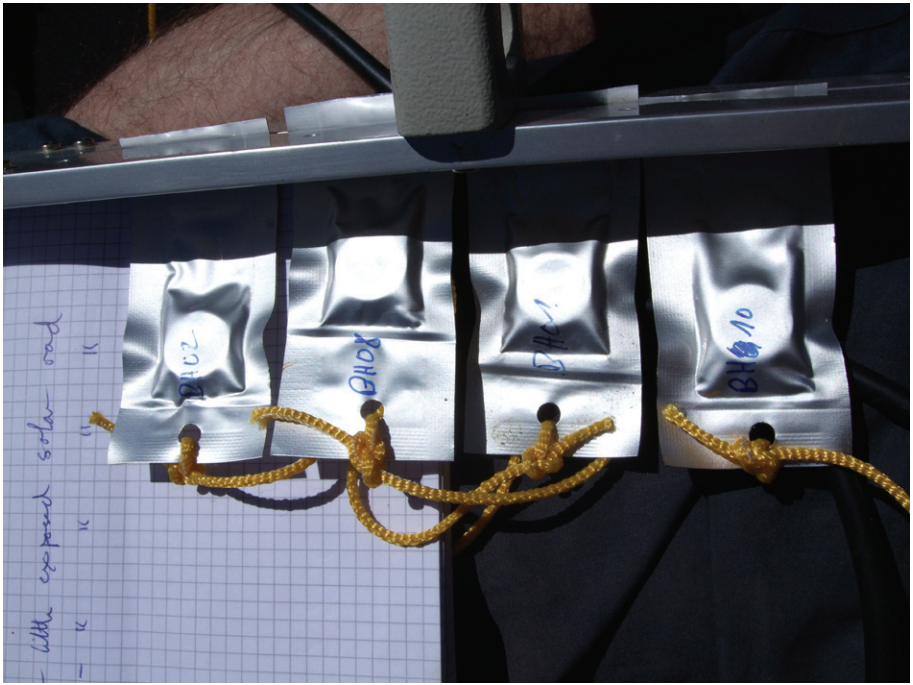

Fig. 2. iButtons were waterproofed by sealing them in plastic pouches with a portable impulse tong sealer. A yellow string was used to refind the individual iButton and to attach them to large boulders to prevent them from falling down steep slopes.

TCD
5, 307–338, 2011

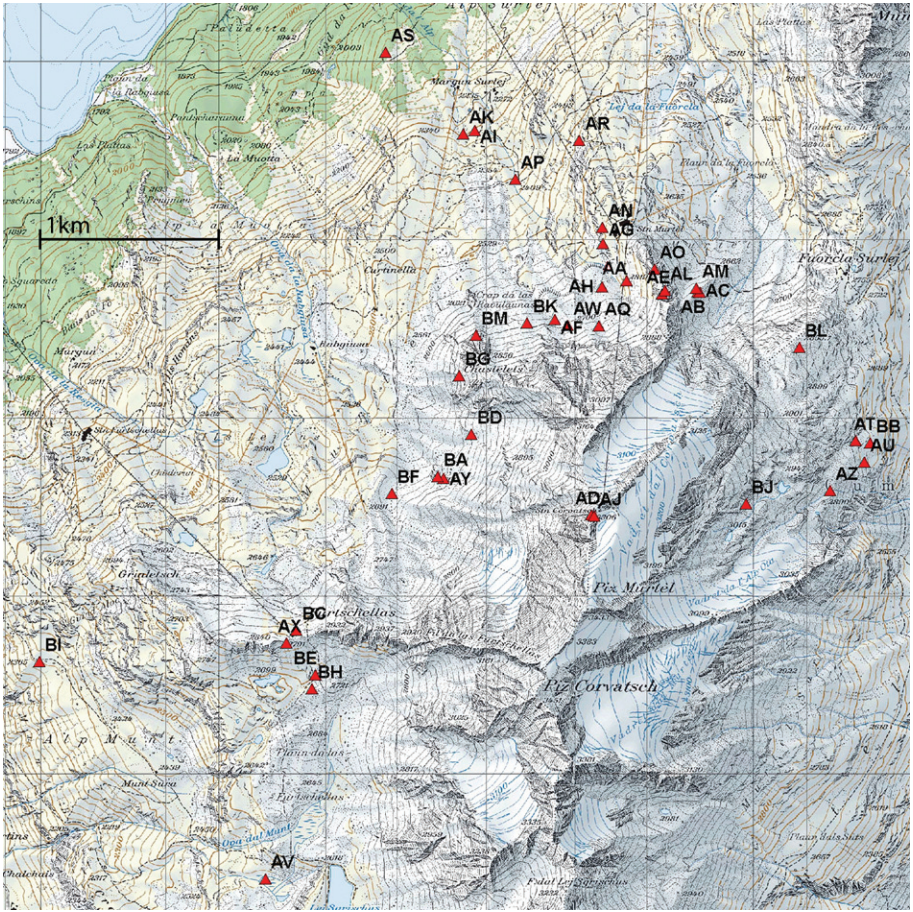

Fig. 3. Locations of the 39 footprints at Corvatsch study site.

TCD
5, 307–338, 2011

Scale-dependent ground surface temperature variability

S. Gubler et al.

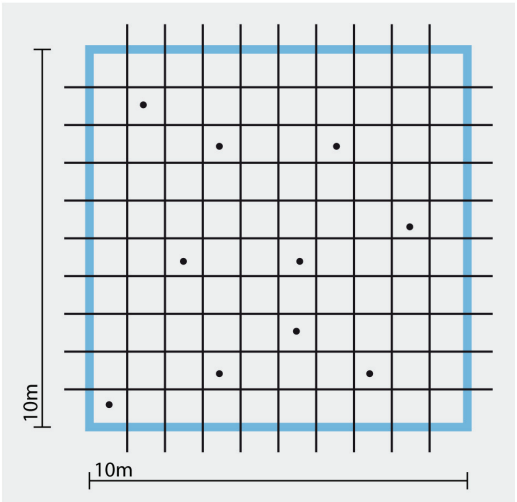

Fig. 4. Ten iButtons were randomly distributed in each 10 m×10 m footprint. One vertex of the square was marked with a stick. Two ropes representing two orthogonal edges were attached to the stick. The blue ropes served as rulers. The local grid and the sampled numbers were manually recorded.

TCD
5, 307–338, 2011

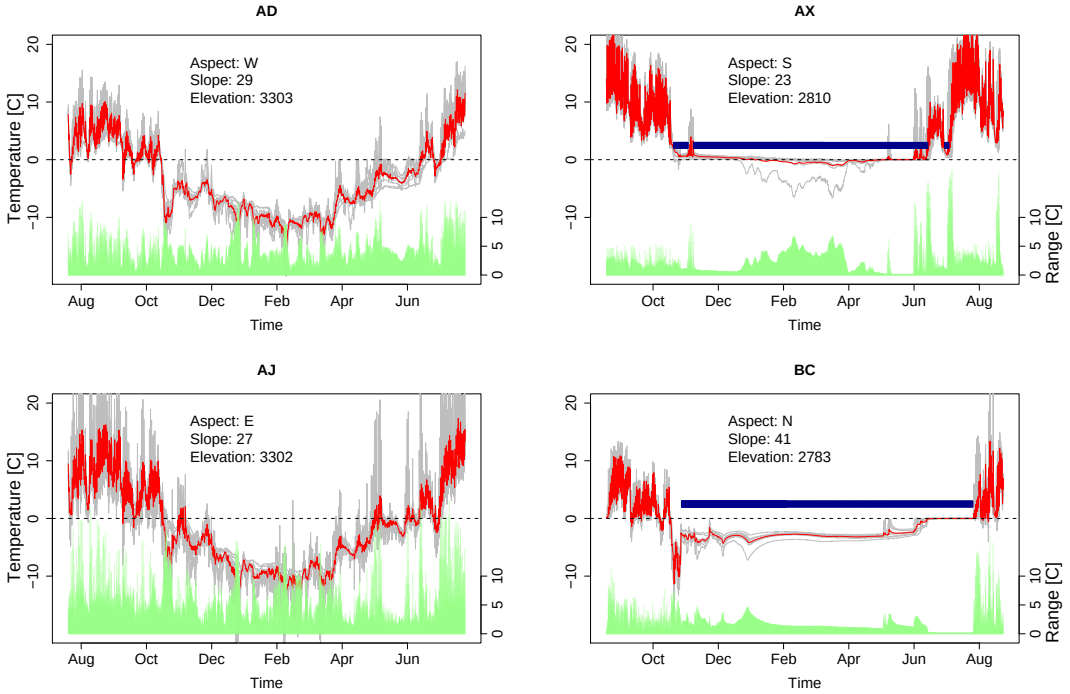

Fig. 5. GST of footprints AD, AJ, AX and BC. Grey lines indicate the individual iButtons, the mean of each time step is plotted in red. At the bottom, the standard deviation at each time step is plotted in green. The blue bar on top of the temperatures indicates the estimated snow cover. Zero curtains can be identified at the end of the snow periods at AX and BC.

TCD
5, 307–338, 2011

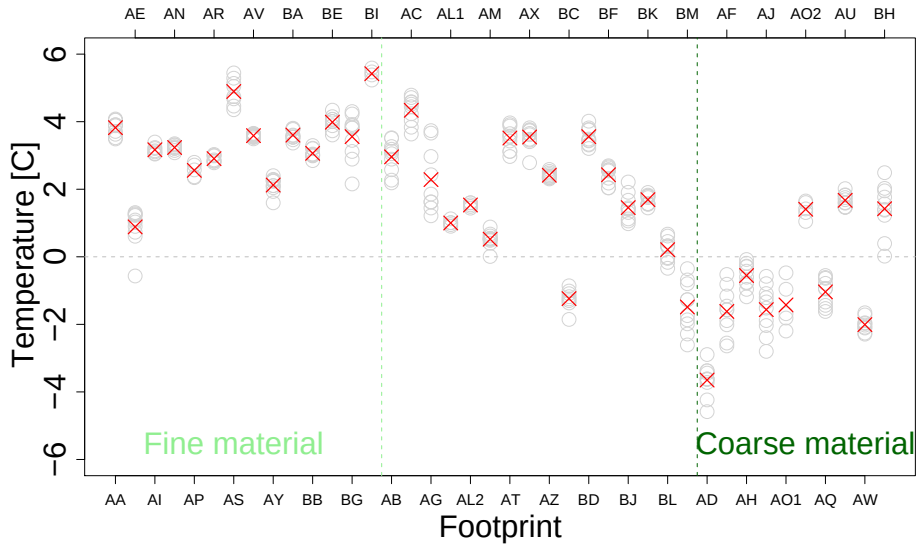

Fig. 6. MAGST of each footprint. The grey circles show each individual iButton, the red cross indicates the mean of all iButtons within one footprints. The footprints are ordered according to the ground cover types.

TCD
5, 307–338, 2011

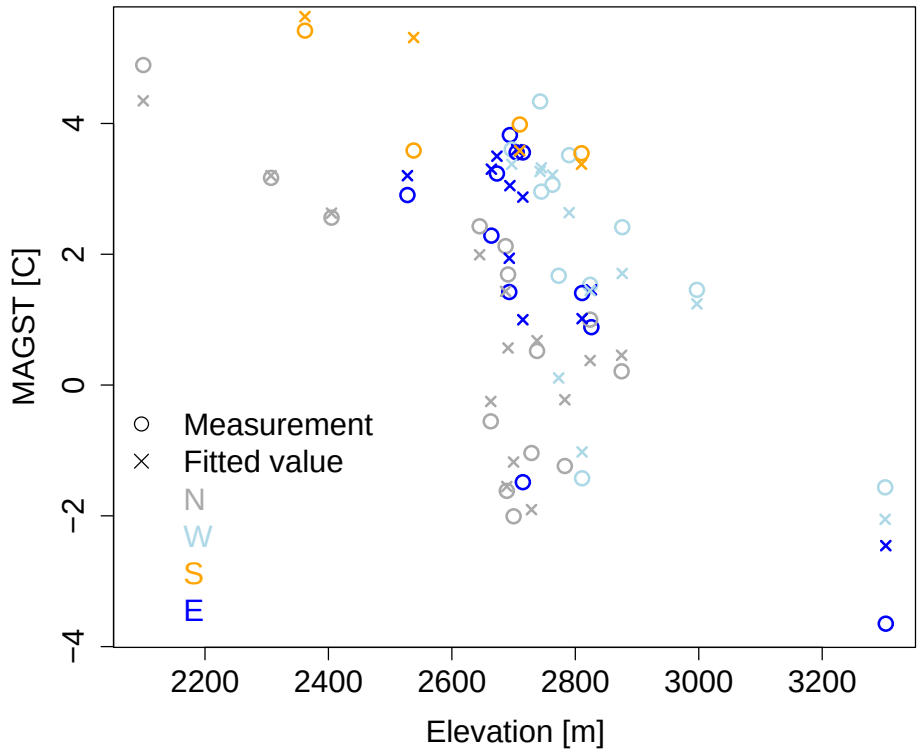

Fig. 7. MAGST of all footprints plotted against elevation. Colors identify the different aspects. Measured MAGST are indicated with a circle, the crosses denote the fitted values from the linear model shown in Eq. (3).

TCD
5, 307–338, 2011

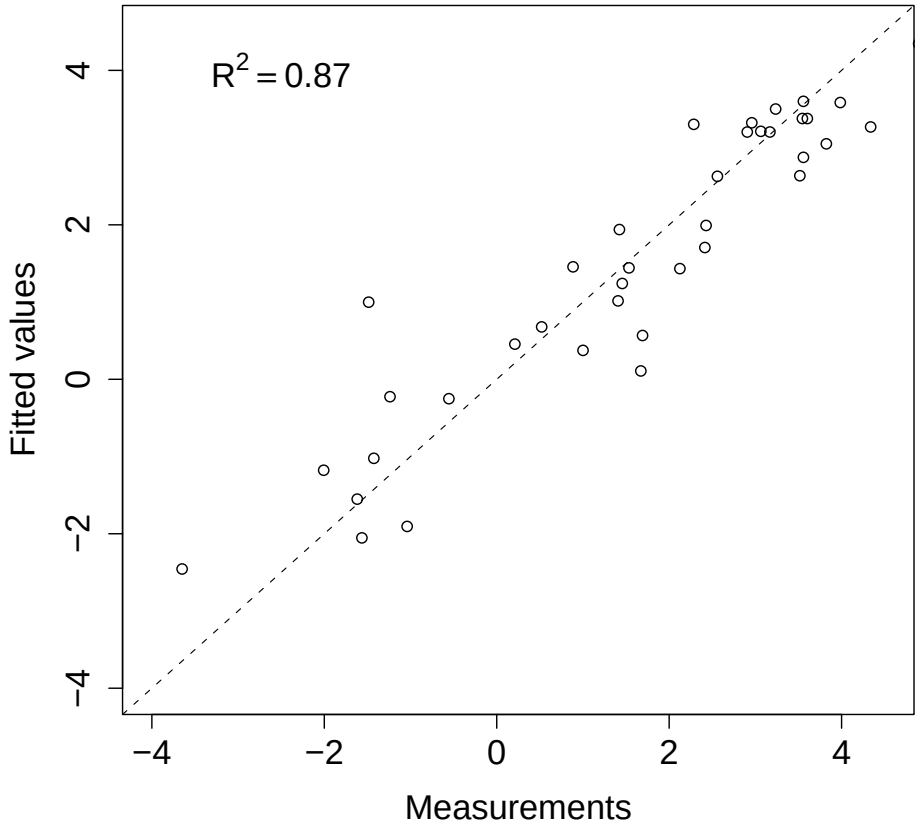

Fig. 8. Scatterplot of measured and fitted MAGST of Model (Eq. 3). The dashed line indicates the diagonal $y=x$. The model explains 87% of the variability of measured MAGST.

TCD
5, 307–338, 2011